Boundary Extraction in Thermal Images by Edge Map

Quming Zhou[*]   Zhuojing Li[**]   J.K.Aggarwal[*]

*Department of Electrical & Computer Engineering
University of Texas at Austin, Austin, TX78731
zhou@ece.utexas.edu
aggarwaljk@mail.utexas.edu

** Department of Computer Science
Texas State University - San Marcos
San Marcos, TX78666, U.S.A
zl1003@swt.edu

ABSTRACT

Extracting object boundaries in thermal images is a challenging task because of the amorphous nature of the images and the lack of sharp boundaries. Classical edge-based segmentation methods have the drawback of not connecting edge segments to form a distinct and meaningful boundary. Many level set approaches, which can deal with changes of topology and the presence of corners, have been developed to extract object boundaries. Previous researchers have used image gradient, edge strength, area minimization and region intensity to define the speed function. Our approach uses edge direction and magnitude, called an edge map, as the main component of the speed function. The edge map points toward the nearest boundary; its magnitude represents the total gradient energy in the half plane. The experimental results are significantly superior to those obtained using edge magnitude alone.

Categories and Subject Descriptors

I. 4.6 [**Image Processing and Computer Vision**]: Segmentation – *edge and feature detection, pixel classification, region partitioning.*

Keywords

Image Segmentation, Boundary, Thermal Image, Level Set, Edge Map and Edge Direction

1. INTRODUCTION

Thermal images are used in many fields, including surveillance, medical diagnostics, fire fighting and non-destructive testing. A number of factors must be considered when analyzing thermal images: the color map, the base temperature and the range of temperature. One distinction between the visual image and the thermal image is the color map. The thermal image camera records the differences in the radiation intensity of objects and maps them in the form of a particular color map. The colors are simply a visual aid to show the temperature differences in each image. In general, it is incorrect to assume that a particular color means warmer or cooler. A thermal image is basically an index image with a special color map. Finding object contours in thermal images is a challenging task because of the amorphous nature of the image and its lack of shape boundaries. As far as we know, very few approaches have been developed using the object boundary to process thermal images.

In this paper, we propose a level set approach to extract interesting object boundaries in thermal images. A review by Suri, *et al.,* [12] lists four kinds of speed functions used in the general level set methods: image gradient, edge strength, area minimization and curvature. However, no paper mentions the edge/gradient direction.

Our approach is based on the direction and magnitude of the edges of the given image. Unlike visual images, object boundaries in thermal images may be broken or may vary significantly when we transform thermal images into intensity images. Edge detection approaches are not suitable for segmenting thermal images [2]. They will detect edges that are not part of an object's boundary or miss parts of a boundary when the intensity contrast is weak. In general, additional effort is needed to connect the incomplete edges into a distinct and meaningful object boundary.

Several search approaches have been proposed to extract object boundaries in images using closed curves. Roughly speaking, there are two types of boundary search approaches. One uses a closed contour represented by a parameterized curve. The problem of finding the desirable contour is posed as an energy minimization problem. The classical Euler-Lagrange formulation of the active contour is called 'snake' [7]. This kind of method relies on an initial guess of the boundary, image features and parameters. Moreover, it suffers from the change of topology and the presence of corners. To overcome these problems, the level set approach has been proposed [10]. The guiding principle of level set methods is to describe a closed curve r in R^2 as the

zero level set of a higher dimension function $\Phi(x,y,t)$ in R^3. Instead of propagating the curve r directly, we consider the evolution of function $\Phi(x,y,t)$ with a speed function F and extract the zero level set of points to obtain the boundary curve. Since level set methods represent the curve in an implicit form, they greatly simplify the management of the contour evolution, especially for handling topological changes. Most of the challenges in level set methods result from the need to construct an adequate model for the speed function.

We propose a segmentation method using a level set to extract objects in thermal images. The edge map is employed instead of the gradient flow. The curve speed function can be adjusted based on the edge map direction as well as the gradient magnitude. Other researchers have used only gradient magnitudes, whereas we use both magnitude and direction. Our method requires only three or four initial points chosen randomly inside or around the interesting object.

2. BACKGROUND

We consider the generation of a family of contours. Let an initial curve r_0 undergo deformation in a Euclidean plane. $r(x, y, t)$ denotes the family of curves generated by the propagation of r_0 in the outward normal direction $\vec{N}$ with the speed F. We ignore the tangential velocity because it does not influence the geometry of the deformation, but only its parameterization. The curve velocity $r_t(x, y, t)$ is denoted by

$$r_t(x, y, t) = F\vec{N} , \tag{1}$$

where F is a scalar function and $\vec{N}$ is a unit normal vector.

According to the level set method, we can express the closed curve $r(t)$ in an implicit form as

$$r(x, y, t) = \{(x, y) \mid \Phi(x, y, t) = 0\} \text{ or } \Phi(r(t), t)) = 0 . \tag{2}$$

By the chain rule,

$$\Phi_t + \Phi_r \cdot r_t = \Phi_t + \nabla\Phi \cdot F\vec{N} = \Phi_t + \nabla\Phi \cdot F \frac{\nabla\Phi}{|\nabla\Phi|} = 0 ,$$

yielding the movement equation of curves,

$$\Phi_t + F \mid \nabla\Phi \mid = 0 , \text{ with } \Phi(x, y, t = 0) = r_0 . \tag{3}$$

The above motion equation (3) is a partial differential equation in one higher dimension than the original problem. Given the initial value, it can be solved by means of difference operators in a fixed grid via

$$\Phi_{i,j}^{n+1} = \Phi_{i,j}^n - \Delta t \cdot h \cdot (\max(F_{i,j}, 0)\nabla^+ + \min(F_{i,j}, 0)\nabla^-) , \tag{4}$$

where n is the iterative time, h is the grid step, Δt is the time step, $F_{i,j}$ is the speed value of pixel (i, j), $\Phi_{i,j}^n$ is the level value of pixel (i, j) at time n and

$$\nabla^+ = (\max(D^{-x}, 0)^2 + \min(D^{+x}, 0)^2 + \max(D^{-y}, 0)^2 + \min(D^{+y}, 0)^2)^{0.5}$$

$$\nabla^- = (\max(D^{+x}, 0)^2 + \min(D^{-x}, 0)^2 + \max(D^{+y}, 0)^2 + \min(D^{-y}, 0)^2)^{0.5}$$

$$D^{-x} = \Phi_{i,j} - \Phi_{i-1,j} , \qquad D^{+x} = \Phi_{i+1,j} - \Phi_{i,j} ,$$

$$D^{-y} = \Phi_{i,j} - \Phi_{i,j-1} , \qquad D^{+y} = \Phi_{i,j+1} - \Phi_{i,j} .$$

This implementation allows the function Φ to automatically follow topological changes and corners during evolution. The speed function F plays a key role in the level set method. When F is positive, the curve expands; when F is negative, the curve

shrinks. Speed models can be generally classified as edge-based [3, 4, 8], region-based [5, 6, 9] or hybrid [13, 11].

In an edge-based model,

$$F = (a + \varepsilon k) / \mid 1 + \nabla G_\sigma * I \mid^p , \tag{5}$$

where k is the curvature of the curve, a, ε and p are constants and $\mid 1 + \nabla G_\sigma * I \mid^p$ is the edge gradient using a Gaussian filter G_σ. Since the stop criterion is the magnitude of the gradient, the speed slows down at strong edges. The drawback of this model is that it only detects objects with edges defined by strong gradients. F is never small enough to stop the curve evolution in a noisy image and the curve may extend beyond the boundary.

In a region-based model,

$$F = \varepsilon k + \log P(I(x, y) \mid a_{inside}) - \log P(I(x, y) \mid a_{outside}) , \tag{6}$$

where k is the curvature of the curve, ε is a constant, $I(x, y)$ is the intensity of pixel (i, j), and a_{inside} and $a_{outside}$ are the intensity distribution parameters for the inside and outside regions, respectively. The problem with this method is that we have to estimate the intensity distribution of the region; however, the distribution model may degrade in a noisy image.

Our approach uses the edge direction as well as the gradient magnitude. A strong edge can stop the curve evolution by its gradient magnitude. A weak edge can halt the curve by its edge map direction, which points toward the closest boundary. The result of evolution will be a curve that goes through the most homogenous region to fit the object boundary. When the speed function is small, the evolution process ceases.

3. LEVEL SET WITH EDGE MAP

In this section, we first describe how we obtain the edge map and then use it as the main component of the speed function in the level set method.

3.1 Edge Map

The motivation for the edge map comes from the fact that the magnitude of the intensity gradient cannot restrict the level set flow completely and the edge direction will help us localize the edge. We introduce a concept, the edge map, to represent the gradient magnitude and direction. We explore the isotropic and linear characteristics of Gaussian filters to obtain the edge map, which accounts for the local edge gradients and their neighborhood.

A 2D isotropic Gaussian filter with standard deviation σ is applied to the image $I(x, y)$. The smoothed image is denoted by $I_\sigma(x, y)$. Further, the gradient images $g_x(x, y)$ and $g_y(x, y)$ are computed by the first order difference of $I_\sigma(x, y)$ along x-axis and y-axis, respectively. Then, the local edge vector at pixel $s = (x_s, y_s)$ along the orientation θ is a linear combination as

$$\vec{E}(s, \theta) = (g_x(s)\cos(\theta) + g_y(s)\sin(\theta))\angle\theta . \tag{7}$$

where *gx(s)* and *gy(s)* are the gradients for pixel *s* along the x-axis and y-axis, respectively.

$\vec{E}(s,\theta)$ is the local edge vector along the orientation θ. It gives us the local intensity change, which is widely used in edge detectors. Our edge map for pixel *s* is defined by

$$\vec{M}(s) = \int_{\theta'}^{\theta'+\pi} \vec{E}(s,\theta)d\theta . \qquad (8)$$

The integration range parameter θ' is now estimated. Without loss of generality, for the pixel $s = (x_s, y_s)$, we compute the intensity difference with pixel $s' = (x_s + d\cos\theta, y_s + d\sin\theta)$, as

$$Diff(s,\theta) = | I_\sigma(x_s + d\cos\theta, y_s + d\sin\theta) - I_\sigma(x_s + y_s) |, \quad (9)$$
where $d = 5\sigma$.

We assume that $Diff(s,\theta)$ is usually no less than $Diff(s,\theta+\pi)$ when the boundary is a distance *d* away from the pixel *s* in the direction θ. However it is still not enough to know where the boundary is exactly. To quantify the prediction of the boundary, an index $P(s,\theta)$ is assigned to every pixel with the same offset distance, *d*, from the pixel *s* by

$$P(s,\theta) = \frac{Diff(s,\theta) - Diff(s,\theta+\pi)}{Diff(s,\theta) + Diff(s,\theta+\pi)} . \qquad (10)$$

A large index value implies a boundary located in that direction. We choose θ' in order to maximize the integration of $P(s,\theta)$ in the corresponding half plane:

$$\theta' = \arg \max_{\theta'} \int_{\theta'}^{\theta'+\pi} P(s,\theta)d\theta . \qquad (11)$$

The edge map $\vec{M}(s)$ is a vector pointing toward the closest boundary pixel with its magnitude representing the total gradient energy in the half plane. Figure 1 shows an example of the edge map for $\sigma = 1$. Each arrow indicates the magnitude and direction of a pixel. The cycle points are the edge pixels obtained by the Canny edge detector. As we can see, the direction of the edge map points to its nearest boundary as its magnitude varies with the distance from the boundary.

3.2 Speed Function
We define our speed function in the outward normal direction of the curve as

$$F = (c - \varepsilon k) / g(\vec{M}) , \qquad (12)$$

where *c* and ε are constants, *k* is the curvature and $g(\vec{M})$ is a scaling function of the edge map $\vec{M}$. Physically, *c* denotes an expansion term, εk plays the smoothing role and $g(\vec{M})$ is a stop criterion. The value of $g(\vec{M})$ depends on the magnitude of the edge map as well as its direction. We give its formula as follows.

Let θ be the angle between the edge map and the outward normal vector $\vec{N}$. Then,

$$g(\vec{M}) = \begin{cases} 1 + |\vec{M}| & if \cos\theta >= 0 \\ 1 + |\vec{M}|^2 & if -0.5 <= \cos\theta < 0 \\ 1 + (3 \sim 5) |\vec{M}|^2 & otherwise \end{cases}$$

The ability to slow down the speed function varies with the direction of the edge map. An edge map with a low magnitude value in the direction opposite to the outward curve normal direction will have a halting ability comparable to that of the strong edge map. Thus, the speed function has values close to zero near high image gradients or edges.
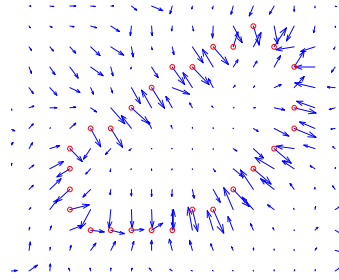

Figure 1: Edge map for each pixel.

4. THERMAL IMAGE SEGMENTATION
The general framework introduced in Section 3 is applied to segment thermal images. Our objective is to construct boundary elements of the given structure in the image.

We tested thermal images from various applications such as medicine, defense and surveillance. We make no assumption about the object's shape, but use only three or four random points inside or around the interesting object as the initial points. Initial pixels locate the place where the evolution begins and provide some gradient information. The use of more initial pixels reduces the total segmentation time but has only a small effect on the final result. In all of our experiments, we use the standard deviation of the smoothing Gaussian filter, $\sigma = 1$; search distance $d = 5\sigma = 5$; grid step $h = 1$; iteration time step $\Delta t = 0.1$; term of the speed function, $c - \varepsilon k = 1 - 0.1k$.

4.1 Examples of Thermal Images
Segmenting thermal medical images is a means of identifying diseased tissues [1]. Once diseased tissue has been segmented, it is useful to compare it with the normal tissue to see how it changes with pathology. For example, utilization of thermal imaging has been an effective method in the evaluation of vascular disease. Fig. 2 shows a patient with vascular disease of the legs. The increased flow of blood through the vessel produces more heat, which is recordable with a thermal imaging procedure. Thermal imaging provides clues to the potential of developing vascular disease which may lead to stroke or cancer. An unsatisfied result is shown in Fig. 2(f) with a general level set method proposed by [4]. The speed function without gradient directions can not maintain the curve along the object boundary.

Fig. 3(a) shows the segmentation of a thermal image of a rat and four calibrating emitters. The four circles correspond to four emitters (only three are really apparent) at different temperatures, and the oblong shape is a live rat. The variability in shape adds to the segmentation challenge. The purpose of this experiment is to measure the thermal temperature of the rat. Fig. 3(b) shows the boundaries of a mouse and the four thermal emitters. The efficacy of this technique is really phenomenal, since using an edge operator on the image yields nowhere near a complete contour for the fourth emitter.

Fig. 4(a) shows an image taken from a sensor mounted on a helicopter. The result shows an example that our approach captures the corners. Fig. 4(b) demonstrates how our approach deals with noisy parts in the object. The curve flows around the noisy parts, because the curve always looks for the relatively homogenous region around its current position. After being isolated by the curve, the noisy parts are removed. This process implies that the curve 'knows' where the noisy parts are during its propagation. The result of our method is shown in Fig. 4(d). The computed boundary captures the corners faithfully. In contrast, snake-based approaches tend to smooth the corners of solid objects. The boundary resulting from the snake proposed by Kass *et.al.,* [7] is shown in Fig. 4(f), with the initial boundary shown in Fig. 4(e). The final boundary produced by the snake approach looks too smooth because the first and the second derivatives are used as constraints in the classical snake [7]. Two more examples on tanks are presented in Fig. 5.

4.2 Approach Comparison

We emphasize the importance of the gradient direction in the speed function. The introduction of the gradient direction as defined here, overcomes the disadvantages in the general level set methods that are summarized in [12].

a) The speed function may not turn out to be zero in multiple objects segmentation.
Fig.3 (a) shows a thermal image of a rat and four circular calibration emitters with very different intensities. The speed function of the brighter emitters can easily be reduced to zero while the dark emitters with low contrast from the background are likely to be missed by the evolving curve under the same model parameters. The active contour meets another problem in segmenting the rat and emitters, i.e. different shapes. Additional care must to be taken to set different model parameters for the rat and emitters. In contrast, our proposed method segments all five objects using the same parameters.

b) Embedding the object.
If one object has one or more objects located inside, the general level set method and the active contour will not capture all objects of interest. Our proposed curve flows around the noisy parts or the embedded objects. After being isolated by the curve, the noisy parts or embedded objects are located. This process implies that the curve 'knows' the noisy parts or embedded objects during its propagation. Fig.4(c) shows how the noisy parts are located.

c) Gaps in Boundaries.
Gaps in boundaries are not a problem in the active contour model because the smoothing restriction and internal iterate values

make the contour complete. However, they are a drawback of the level set method when applied to noisy images. The contour in the level set method is in an implicit form, which may simply leak through gaps.

5. CONCLUSIONS

In this paper we have presented a level set approach to segment thermal images. The edge map is introduced as the main component of the speed function. The edge map points toward the nearest boundary and its magnitude represents the total gradient energy in the half plane. The proposed approach uses both the edge direction and the gradient magnitude to overcome the problems resulting from weak edges. The results are significantly superior than results obtained using edge magnitude alone. As shown in our experiments, our approach has several desirable features besides those of the general level set method. Good boundaries can be extracted from thermal images with very few initial pixels inside or around the object; the final result is relatively independent of the initial guess; adding more initial pixels can reduce the total segmentation time; the parameters we set in our experiments can work for thermal images from various applications; and the curve 'knows' where the noisy parts are.

Figure 2(a)   Figure 2(b)

Figure 2(c)   Figure 2(d)
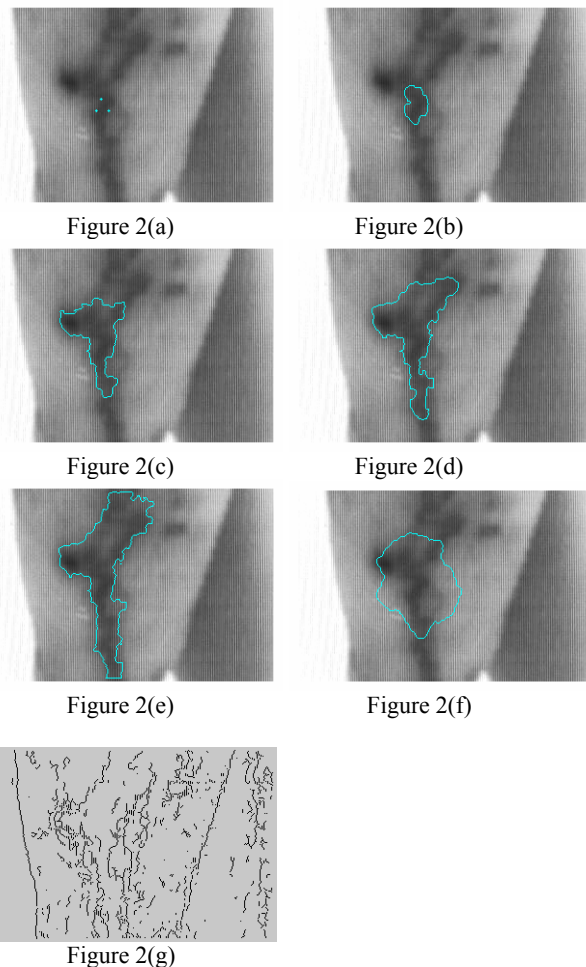

Figure 2(e)   Figure 2(f)

Figure 2(g)

Figure 2: (a) Three initial pixels. (b-d) Evolution of the boundary. (e) Final segmentation result. (f) Evolution without considering gradient directions. (g) The Canny edges
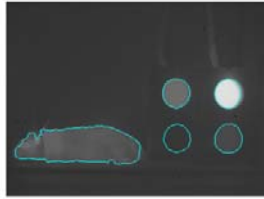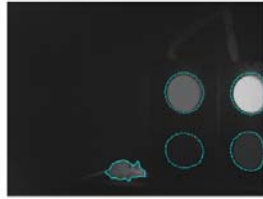
Figure 3(a)   Figure 3(b)

Figure 3: (a) Segments of a thermal image of a rat and four calibrating emitters (only three are visible). (b) Segments of a mouse and emitters.
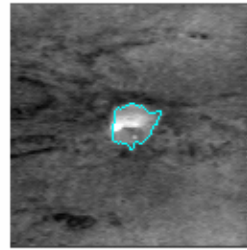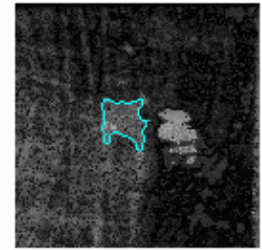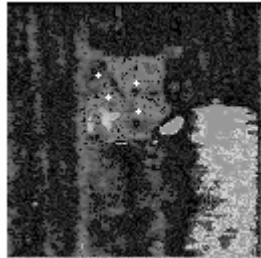

Figure 4(a)   Figure 4(b)
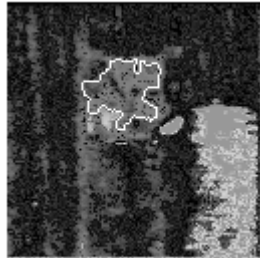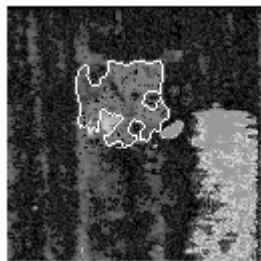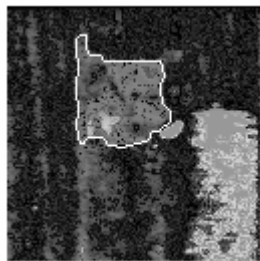

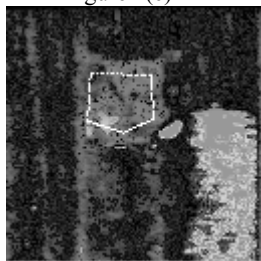Figure 4(c)   Figure 4(d)

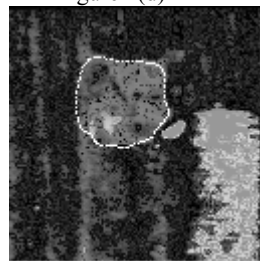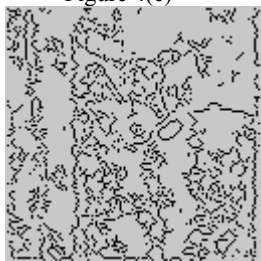Figure 4(e)   Figure 4(f)

Figure 4(g)

Figure 5: (a) Four initial pixels in a M60 main battle tank. (b-c) Evolution of the curve with noise parts in the object. (d) The final result. (e) The initial boundary for the snake. (f) The boundary using the snake. (g) The Canny edges

Figure 5(a)   Figure 5(b)

Figure 5: Two tank images.

6. REFERENCES

[1] K. Ammer, P. Melnizky, O. Rathkolb and E. F. Ring. Thermal Imaging of Skin Changes on the Feet of Type II Diabetics. *Proc. Int. Conf. on EMBS*, vol. 3, pp. 2870-2872, Istanbul, Turkey, Oct. 2001.

[2] J. Canny. A Computational Approach to Edge Detection. *IEEE Trans. PAMI*, vol. 8, 679-698, Nov. 1986.

[3] V. Caselles, F. Catte and F. Dibos. A Geometric Model for Active Contour in Image Processing. *Numerische Mathematik*, vol. 66, no. 1, pp. 1-31, 1993.

[4] V. Caselles, R. Kimmel and G. Sapiro. Geodesic Active Contour. *Proc. Int. Conf. on Computer Vision,* pp. 694-699, Boston, MA, 1995.

[5] T. F. Chan and L. A. Vese. Active Contour without Edges. *IEEE Trans. Image Processing*, vol. 10, no. 2, pp. 266-277, Feb. 2001.

[6] E. Debreuve, M. Barlaud, G. Aubert, I. Laurette and J. Darvourt. Space-Time Segmentation using Level Set Active Contours Applied to Myocardial Gated SPECT. *IEEE Trans. Medical Imaging*, vol. 20, no. 7 pp. 643-659, July 2001.

[7] M. Kass, A. Witkin and D. Terzopoulos. Snake: Active Contour Models. *Int. J. Comput. Vis.*, vol. 1, pp.321-331, 1987.

[8] R. Malladi, J. A. Sethian and B. C. Vemuri. Shape Modeling with Front Propagation: A Level Set Approach. *IEEE Trans. PAMI,* vol. 17, no. 2, pp. 158-175, Feb. 1995.

[9] A. Mansouri. Region Tracking via Level Set PDEs without Motion Computation. *IEEE Trans. PAMI*, vol. 24, no.7, pp. 947- 960, July 2002.

[10] S. Osher and J. A. Sethian. Front Propagation with Curvature-dependent Speed: Algorithms Based on Hamilton-Jacobi Formulation. *J. Computat. Phys.,* vol.79, pp.12-49, 1988.

[11] N. Paragios and R. Deriche. Geodesic Active Contours and Level Sets for the Detection and Tracking of Moving Objects. *IEEE Trans. PAMI*, vol. 22, no.3, pp. 266-280, March 2000.

[12] J. S. Suri, K.Liu, S. Singh, S.N.Laxminarayan, X.Zeng and L.Reden. Shape Recover Algorithms Using Level Sets in 2-D/3-D Medical Imagery: a State-of-the-Art Review. *IEEE Trans. Information Technology in Biomedicine*, vol.6, no.1, pp.8-28, March 2002.

[13] S. C. Zhu and A. Yuille. Region Competition: Unifying Snakes, Region Growing, and Bayes/MDL for Multiband Image Segmentation. *IEEE Trans. PAMI*, vol. 18, no.3, pp. 884-900, Sept. 1996.

258